Boundary-Layer Meteorol (2010) 137:307–326
DOI 10.1007/s10546-010-9529-5

RESEARCH NOTE

Determining the Oxygen Isotope Composition of Evapotranspiration Using Eddy Covariance

T. J. Griffis · S. D. Sargent · X. Lee · J. M. Baker · J. Greene · M. Erickson · X. Zhang · K. Billmark · N. Schultz · W. Xiao · N. Hu

Received: 1 March 2010 / Accepted: 13 July 2010 / Published online: 30 July 2010

Abstract The oxygen isotope composition of evapotranspiration (δ_F) represents an important tracer in the study of biosphere–atmosphere interactions, hydrology, paleoclimate, and carbon cycling. Here, we demonstrate direct measurement of δ_F based on the eddy-covariance and tunable diode laser spectroscopy (EC-TDL) techniques. Results are presented from laboratory experiments and field measurements in agricultural ecosystems. The field measurements were obtained during the growing seasons of 2008 and 2009. Water vapour mixing ratios (χ_w) and fluxes (F) were compared using EC-TDL and traditional eddy-covariance and infrared gas analyser techniques over a soybean canopy in 2008. The results indicate that χ_w and F agreed to within 1 and 6%, respectively. Measurements of δ_F above a corn canopy in 2009 revealed a diurnal pattern with an expected progressive ^{18}O enrichment through the day ranging from about $-20‰$ before sunrise to about $-5‰$ in late afternoon. The isotopic composition of evapotranspiration was similar to the xylem water isotope composition ($\delta_x = -7.2‰$) for short periods of time during 1400–1800 LST, indicating near steady-state conditions. Finally, the isotopic forcing values (I_F) revealed a diurnal

T. J. Griffis (✉) · M. Erickson · K. Billmark · N. Schultz
Department of Soil, Water, and Climate, University of Minnesota-Twin Cities,
Saint Paul, MN, USA
e-mail: tgriffis@umn.edu

S. D. Sargent · J. Greene
Campbell Scientific Inc., Logan, UT, USA

X. Lee · X. Zhang
School of Forestry and Environmental Studies, Yale University,
New Haven, CT, USA

J. M. Baker
Agricultural Research Service, United States Department of Agriculture,
Saint Paul, MN, USA

W. Xiao · N. Hu
School of Applied Meteorology, Nanjing University of Information Science and Technology,
Nanjing, Jiangsu, China

pattern with mean maximum values of $0.09\,\mathrm{m\,s^{-1}}$ ‰ at midday. The I_F values could be described as an exponential relation of relative humidity confirming previous model calculations and measurements over a soybean canopy in 2006. These patterns and comparisons indicate that long-term continuous isotopic water vapour flux measurements based on the eddy-covariance technique are feasible and can provide new insights related to the oxygen isotope fractionation processes at the canopy scale.

Keywords Eddy covariance · Evapotranspiration · Isotopic discrimination · Isotopic forcing · Oxygen isotopes · Tunable diode laser spectroscopy · Water vapour

1 Introduction

The isotopic composition of atmospheric water vapour represents an important environmental tracer that can be used to better understand the complex physical and biophysical processes involved in land-atmosphere transport of water. The turbulent transport of water vapour between the hydrosphere / biosphere and atmosphere represents the dominant energy sink for the radiant energy absorbed at the Earth's surface, but its influence on the atmosphere's water vapour isotopic budget remains poorly understood (Lee et al. 2005; Worden et al. 2007). A considerable amount of isotope research has focused on the condensed phase. However, the analysis of water vapour isotopic composition has been limited to relatively short-term (i.e. less than a few weeks) campaigns. The only exceptions are the 8-year record (1981–1988) of Jacob and Sonntag (1991) who collected and measured water vapour content once every 24 or 48 h and Angert et al. (2008) who measured water vapour content collected two times per week over a 9-year period (1998–2006). Far fewer studies have attempted to quantify the isotope composition of the water vapour flux (Lee et al. 2007; Lai et al. 2006; Yakir and Wang 1996; He and Smith 1999). This limitation has long been recognized as an impediment to improved understanding of the water vapour isotope budget, and the cycling of atmospheric moisture. Progress has been limited by a lack of suitable in situ methodologies that can be deployed in the field. However, laser-based technologies are rapidly becoming available so that these measurements will likely be routine in the near future (Lee et al. 2005; Wang et al. 2009; Sturm and Knohl 2009).

These new optical isotope methods have the potential to provide near-continuous and fast (≈10 Hz) measurements of isotopic water vapour mixing ratios. The high temporal resolution provides a unique opportunity to directly quantify the water vapour isoflux and atmospheric isoforcing (Lee et al. 2007, 2009; Griffis et al. 2008; Welp et al. 2008). These developing technologies may provide a critical link to upper tropospheric observations of isotopic water vapour based on satellites (Worden et al. 2006, 2007; Herbin et al. 2007; Brown et al. 2008). Worden et al. (2007) used the Tropospheric Emission Spectrometer sensor on board NASA's Aura satellite to study the transport and cycling of tropospheric water vapour. We anticipate that the coupled application of ground-based optical isotope and satellite observations will provide new insights into the links between boundary-layer and upper troposphere processes, and should provide critical data for interpreting variations in atmospheric $C^{18}O^{16}O$ (Welp et al. 2008; Xiao et al. 2010).

Quantifying land-atmosphere water vapour and carbon isotope exchange has been limited to a number of indirect methodologies including relaxed eddy accumulation, the eddy-covariance/flask isotope method, and the flux-gradient technique (Bowling et al. 1999, 2001; Yakir and Wang 1996; Griffis et al. 2004, 2005; Lee et al. 2005). More recently we demonstrated that it was possible to measure the isotopic fluxes of CO_2 directly using

eddy-covariance and tunable diode laser spectroscopy (Griffis et al. 2008). The eddy-covariance method has several advantages over these other techniques and is already widely used within the Global Fluxnet network (now consisting of more than 500 sites). Despite the simple theory and few underlying assumptions, the eddy-covariance method is technically demanding and requires a fast-response analyser that is stable over the typical averaging period.

In this paper we describe a lead-salt tunable diode laser (TDL) spectroscopy system (TGA200, Campbell Scientific Inc., Logan, Utah, USA) and the eddy-covariance (EC) application (EC-TDL approach) for water vapour isotopic flux measurements. A similar system (TGA100, CSI) was first used by Lee et al. (2005) to measure isotopic water vapour mixing ratios in a flux-gradient mode. The system described here represents a redesign specific for eddy-covariance flux measurements. Further, we build on the recent eddy-covariance CO_2 isotope technique described in Griffis et al. (2008) and highlight the technical details related to the water vapour isotope application.

2 Basic Theory

Briefly, the total water vapour flux (F, mmol m^{-2} s^{-1}) between the biosphere and atmosphere can be obtained from,

$$F = \bar{\rho}_a \overline{w' \chi_w'} + S = \bar{\rho}_a \int C_{w\chi_w}(f) df + S, \tag{1}$$

where, $\bar{\rho}_a$ is the molar density of dry air, w is the vertical wind velocity, χ_w is the total H_2O molar mixing ratio, the primes indicate the differences between instantaneous and mean values and the overbar indicates an averaging operation (i.e. 30-min integration period). Here $\overline{w' \chi_w'}$ is the covariance of w and χ_w and is equivalent to the cospectral density of the fluctuations in vertical wind velocity and H_2O mol mixing ratio ($C_{W\chi_w}$), where f is the frequency. The storage term (S) is defined as the rate of change in total H_2O between the ground and the eddy-covariance measurement height.

Similarly, the isotopic water vapour fluxes can be determined from,

$$F^x = \bar{\rho}_a \overline{w' \chi^x{}' w'} + S^x = \bar{\rho}_a \int C^x_{w\chi_w}(f) df + S^x, \tag{2}$$

where superscript x indicates one of the isotopologues ($H_2^{16}O$ or $H_2^{18}O$).

The isotopic composition of the water vapour flux can be determined from the flux ratio,

$$\delta_F = 1000 \left(\frac{F^{18}/F^{16}}{R} - 1 \right) \tag{3}$$

with the isotope ratio reported relative to R, the Vienna Standard Mean Ocean Water scale. Further, these high frequency measurements provide an opportunity to explore the cospectral flux ratio as a function of eddy frequency. This technique may lead to new process information regarding the source origin of water vapour in turbulent transport and in boundary-layer flows,

$$\delta_F(f) = 1000 \left(\frac{C^{18}_{w\chi_w}(f)/C^{16}_{w\chi_w}(f)}{R} - 1 \right). \tag{4}$$

Finally, the impact on the isotopic composition of surface-layer air can be determined from the isotopic forcing (I_F) principle (Lee et al. 2009),

$$I_F = \overline{w'\delta'_v} = \frac{F}{C_w}(\delta_F - \delta_v) \tag{5}$$

where $\overline{w'\delta'_v}$ represents the mean covariance between w and the oxygen isotope composition of water vapor (δ_v) (m s^{-1} ‰) and C_w is water vapour molar concentration expressed here in units of mmol m^{-3}.

3 Methodology

3.1 Research Site and Experiments

Experiments were conducted in the laboratory and at the Rosemount Research and Outreach Center at the University of Minnesota from August 8 (DOY 221) to September 19 (DOY 263), 2008 and June 19 (DOY 170) to August 31 (DOY 243), 2009. The research site is part of the AmeriFlux network and is located about 25 km south of Saint Paul, Minnesota, USA. The field site is currently managed in a conventional corn/soybean rotation. In this study the measurements were made during the soybean (*Glycine max*, C_3 photosynthetic pathway) phase of the rotation (2008) and during the corn (*Zea mays*, C_4 photosynthetic pathway) phase (2009). The eddy-covariance system was located approximately 50 m from the northern edge of the research field, with southerly winds producing an upwind fetch of about 350 m. The TDL system was located about 1.5 m from the micrometeorological tower and was exposed to the weather elements. $H_2^{16}O$ and $H_2^{18}O$ absorption were measured at wavenumbers of 1500.546 and 1501.188 cm^{-1}, respectively. The design modifications of the TDL system included matching the sample and reference cells in size (1.466 m path length, 300 ml volume), which are now constructed from a graphite composite. These modifications were made to help reduce pressure broadening effects (a source of non-linearity) and to improve temperature stability. Our experiments in 2008 focused on comparing the frequency response, total water vapour mixing ratio, and total water vapour eddy fluxes of the EC-TDL system versus traditional infrared gas analysis (IRGA, open and closed-path systems). In 2009 the EC-TDL experiments focused on examining the isotopic composition of water vapour mixing ratios and fluxes with detailed comparisons with the isotope composition of soil and plant xylem water.

3.2 Tunable Diode Laser Calibration and Air Sampling

A bubbler device was used to provide the TDL water vapour reference gas at approximately 12 ml min^{-1} (Fig. 1). This device differs from that used by Lee et al. (2005) who provided a pure source of water vapour by sampling the head space air volume of a water reservoir maintained at a temperature of 40°C. Here we saturated an air stream at a set-point temperature of 45°C and at an atmospheric pressure of approximately 98.5 kPa to produce a water vapour mixing ratio of 110 mmol mol^{-1}. Ambient air was filtered and pulled into the bottom of a glass bottle where it bubbled to the surface. Air was pulled from the head space using a short tube with a flow restriction (0.2 mm inner diameter and 100 mm length), and which was immersed in the water and connected to the TDL reference cell at 1.2 kPa. This prevented condensation from occurring inside the bubbler device. Further, the reference water was enriched in ^{18}O by mixing 10 mg of labeled H_2O (95% ^{18}O content) (Cambridge Isotope

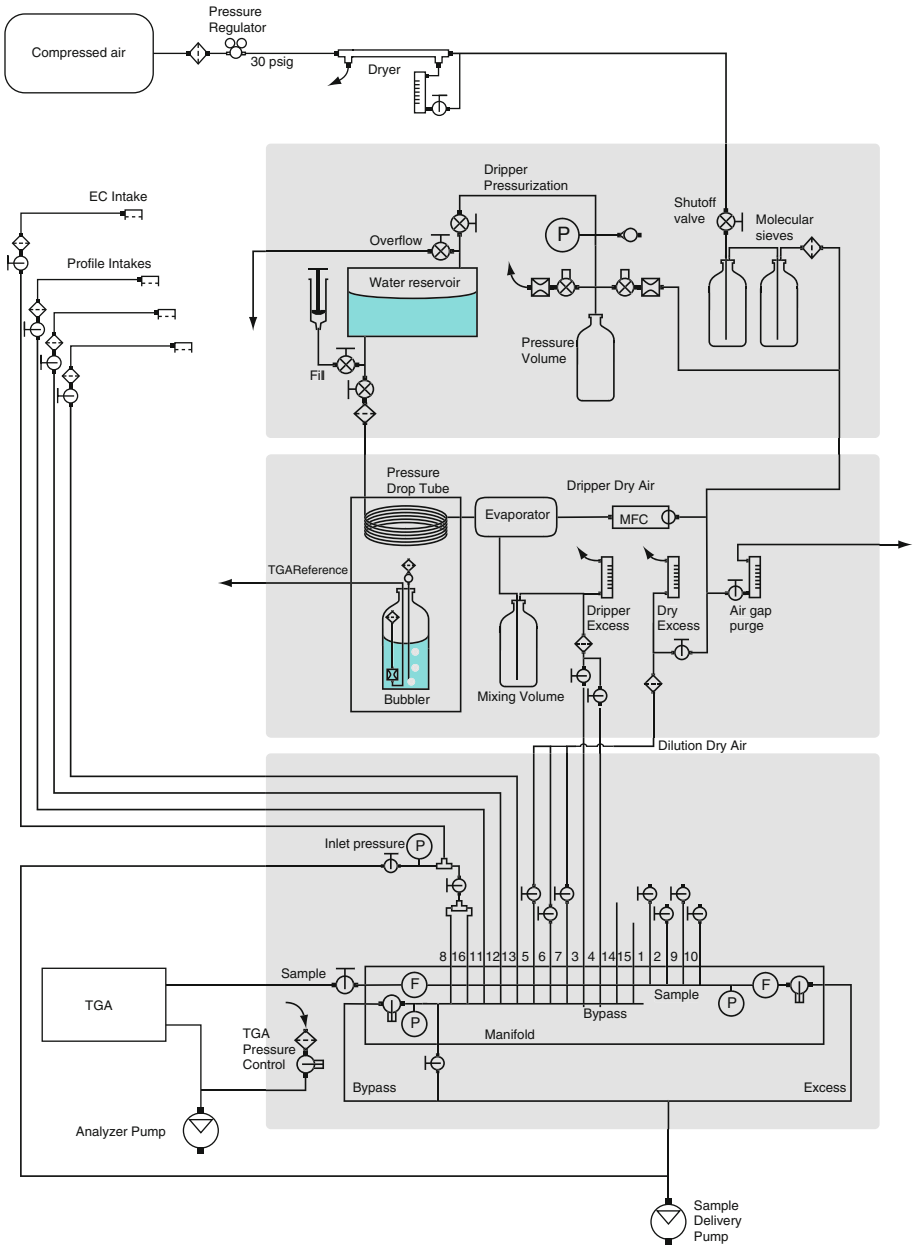

Fig. 1 Diagram of the eddy-covariance and tunable diode laser water vapour sampling system

Laboratories, Andover, Maine, USA) into 200 ml of standard liquid water. This resulted in approximately equal effective absorption line strengths for each isotope.

The calibration strategy is based on generating different water vapour span values having identical isotope ratios using a dripper evaporation technique. Here, we assume that the total water vapour mixing ratio measured by the TDL is correct. Lee et al. (2005) developed the

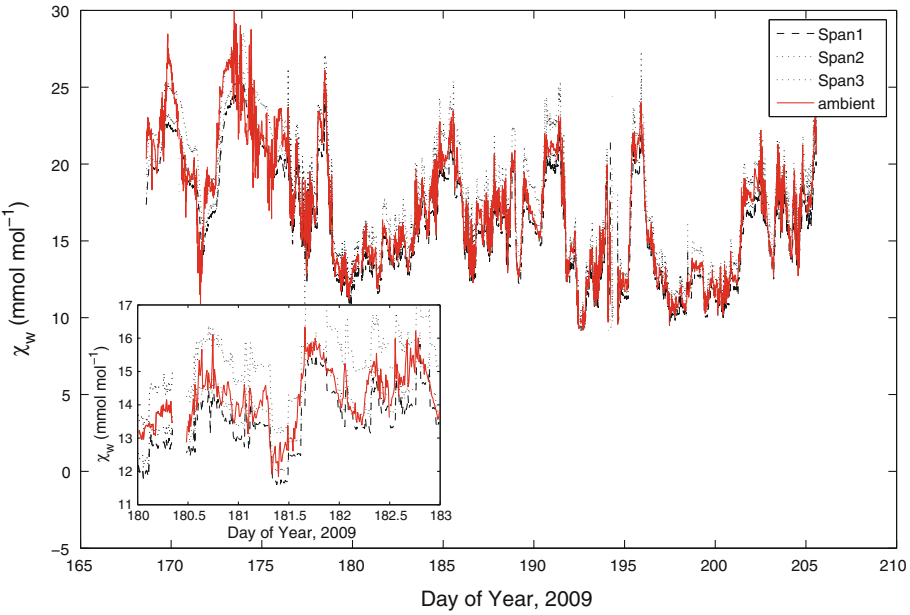

Fig. 2 Time series of the dynamic water vapour mixing ratio calibration for the 2009 corn growing season. Three span values were used to bracket the ambient water vapour mixing ratio by adjusting the pressure set point of the calibration dripper device. The *inset* shows a magnified view of the time series from DOY 180 to DOY 183 where the ambient mixing ratio was bracketed to within 1 mmol mol^{-1}

first dripper system that used a syringe pump. The dripper system used in this experiment consisted of a 650 ml water reservoir treated with ultraviolet radiation to prevent bacterial/fungal growth (Biologic BIO-1.5 ultraviolet purifier, Atlantic Ultraviolet Corp., Sacramento, USA). A constant drip rate was maintained by using a pressure drop laminar flow tube (0.28 mm inner diameter and 6.1 m length), which was connected to the water reservoir that was pressurized via compressed air up to 200 kPa above ambient. This allowed water to displace through the laminar flow tube and drip on to a small heated (116°C) stainless steel evaporating plate. The drip rate could be controlled with pressure over a range that was ultimately determined by the length and diameter of the laminar flow tube. Precise pressure control of the water reservoir was achieved by using a pressure volume with a fill and vent valve that was controlled to a set point by the data logger. The effect of temperature on the viscosity of water had a very minor influence on the drip rate. To reduce such effects, and to eliminate condensation, the temperature of the dripper system was thermostatically controlled. The heated evaporating plate had a shallow channel that allowed the dry air stream to mix with the evaporated water. Further, the heat plate was covered with wicking paper (Whatman grade 3MM chromatography paper, 20 mm, New Jersey, USA) to ensure rapid and complete evaporation of the water droplets. The wicking paper was changed every one to two weeks to prevent the build-up of mineral deposits. The dripper device was filled weekly with laboratory standard water ($\delta^{18}O = -8.4‰$). Its isotopic ratio was measured before and after each refill. In 2009, we used a dynamic calibration technique by spanning ambient water vapour mixing ratio values to within approximately 8% by varying the dripper set-point pressure. Figure 2 shows an example of this dynamic tracking over the period DOY 165–DOY 210, 2009.

Dry air was generated in the field for the dripper calibration device and to provide purge air to eliminate water vapour between the TDL laser source and the reference and sample cells. The dry air (ultra zero) was generated using a three-stage process. First, air was compressed and conditioned using an oil and liquid water trap; second, the compressed air was passed through a nafion dryer (PD1000, Perma Pure Inc., New Jersey, USA) using a split sample flow method; finally, the air was passed through two molecular sieves (Molecular Sieve Zeolite, 13X-Z8, Agilent Technologies, California, USA) that were joined in series. The dry air was pushed through a mass flow controller (MPC0002B, Porter Instrument Co., Pennsylvania, USA) into the evaporator to provide the high span calibration air stream. The high span calibration air was further diluted downstream using the same dry air source and a combination of three valves to produce the desired range of span values.

The air sampling system consisted of a custom designed 16 valve manifold with integrated pressure control via a data logger (CR3000, CSI). In this application the excess flow through the outlet of the manifold was controlled to maintain constant pressure in the manifold and constant flow to the TDL. The TDL sample cell pressure was maintained at 1.1 kPa. All of the sample inlets use an internal bypass to allow constant flow and to reduce the equilibration time following valve switching. This also maintains lower sample line pressure and reduces the potential for condensation. In this field experiment three inlets were used to provide dry air for producing the three span gases described above.

In 2008 four inlets were used for the air sampling. These included the eddy-covariance inlet located at 2.7 m above the soil surface and three profile inlets located at 0.10, 0.85, and 1.85 m. A base flow rate of $10\,\mathrm{l\,min^{-1}}$ was pulled through the eddy-covariance inlet and a base flow rate of $1.7\,\mathrm{l\,min^{-1}}$ was pulled through each of the three profile inlets using a diaphragm pump (1-DOAV502, Gast Manufacturing Inc., Michigan, USA). Each profile inlet was buffered using a 5 l custom-blown glass mixing volume. The base flow was sub-sampled at $1.5\,\mathrm{l\,min^{-1}}$ through the TDL using a vacuum pump (RB0021, Busch Inc., Virginia, USA). The sample inlets were maintained at 65.0 kPa. All of the sample tubing consisted of natural coloured high density polyethylene (HDPE, 6.25 mm outer diameter part number 50375K41, McMaster-Carr, New Jersey, USA) and was heated with heating tape and wrapped with foam insulation to prevent condensation, reduce adsorption, and to improve the overall frequency response of the system.

The valve switching sequence was controlled using the data logger and valve drive module (SDM-CD16S, CSI). In 2008, a 10-min (600 s) sample cycle included the following sequence: (1) calibration with ultra dry air for a period of 30 s; (2) calibration with span 1, span 2, and span 3 for a period of 10 s each; (3) sampling of profile inlets z_1, z_2, and z_3 for a period of 10 s each; (4) sampling the eddy-covariance inlet for a period of 510 s. At the end of the 10-min cycle the sequence was reversed beginning with the high span calibration.

In 2009 the sampling scheme was simplified to include only the eddy-covariance inlet mounted at 3.5 m above the soil surface and the storage term in Eq. 2 was not measured. As discussed by Welp et al. (2008) this is unlikely to have a significant influence on δ_F. Further, our analyses have shown that δ_F is relatively insensitive to using a friction velocity filter, which provides indirect evidence that the storage term is not significant, at least in low stature vegetation. A base flow rate of $12\,\mathrm{l\,min^{-1}}$ was pulled through the system and sub-sampled at $1.5\,\mathrm{l\,min^{-1}}$. The sample inlet was maintained at 60.0 kPa. In this sampling configuration there was a 1.1 s time delay between the sonic anemometer and the water vapour isotope mixing ratio measurement. The majority of this delay (0.744 s) was attributed to the TDL 5 Hz digital filter, see Griffis et al. (2008).

A 12-min (720 s) cycle was used and the sampling sequence consisted of: (1) calibration with ultra dry air for a period of 30 s; (2) calibration with span 1, span 2, and span 3 for

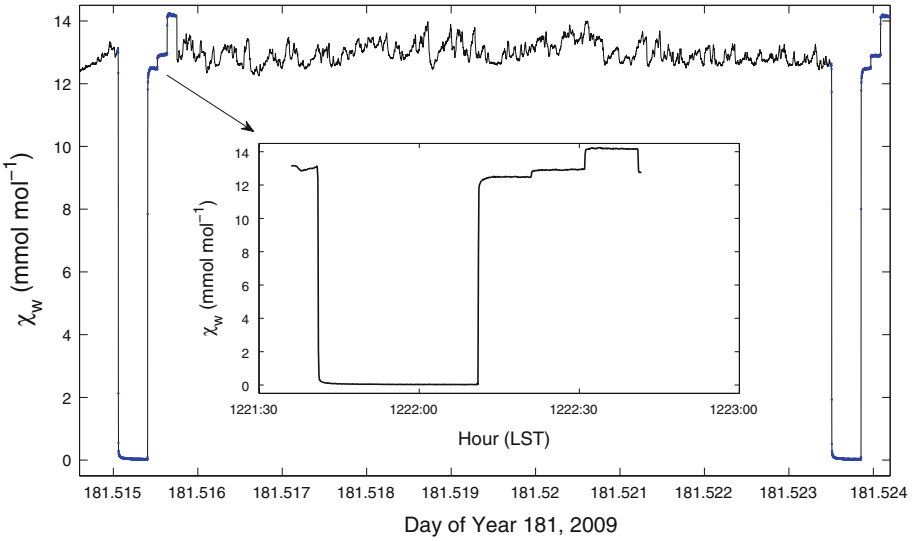

Fig. 3 Transient response following valve switching. The example shown illustrates the valve switching prior and following the ambient air sampling. The *inset* shows a magnified view of the calibration sequence including dry air followed by the three span gas values

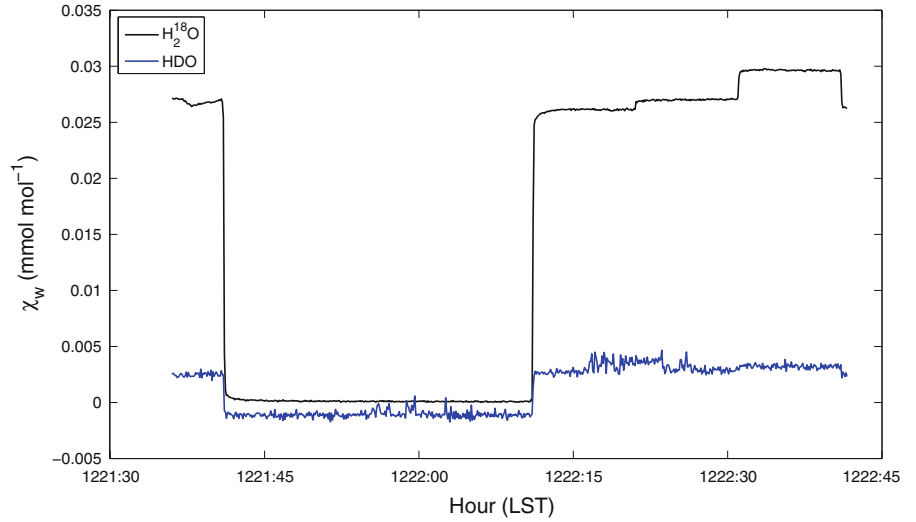

Fig. 4 Same as the inset of Fig. 3, but for $H_2^{18}O$ and deuterium

a period of 10 s each; (3) sampling of the eddy-covariance inlet for a period of 660 s. In post processing, an omit time of 5 s was used following valve switching to ensure that air sample and calibration samples had equilibrated to their respective step change. An omit time of 20 s was required for the ultra dry air calibration. Figure 3 shows an example of the transient response and equilibration time for $H_2^{16}O$ associated with valve switching. Figure 4 illustrates the transient response for the minor isotopes. These data indicate greater noise in the deuterium signal, and what appears to be a stronger tubing effect on

deuterium. Sturm and Knohl (2009) recently examined Teflon and Synflex (a composite of polyethylene/aluminum with an ethylene copolymer internal coating) tube types and their influence on water vapour attenuation and fractionation. They concluded that Synflex had a slower equilibration time and an apparent strong kinetic fractionation effect for deuterium. Our own laboratory tests have shown that natural coloured high density polyethylene (HDPE) tubing performed as well or slightly better than Teflon tubing. Further, when testing Synflex, we confirmed the longer equilibration time compared to HDPE and Teflon. However, we were not able to confirm the strong kinetic fractionation effect for deuterium. Tube attenuation and fractionation effects related to the eddy-covariance measurements are discussed in more detail below.

3.3 Data Acquisition and Post Processing

All raw signals were recorded at 10 Hz using the data logger, with post-processing performed using custom software developed with Matlab (The Mathworks Inc., Natick, MA, USA). The water vapour eddy-covariance and TDL data were processed using a methodology similar to that described in Griffis et al. (2008):

1. Dry (zero) and span values were smoothed and interpolated between calibration intervals at 10 Hz.
2. A zero offset value was removed from the measured isotopic mixing ratios for each span gas and air sample.
3. A correction factor based on the difference between the dripper isotope ratio (standard) and the measured isotope ratio of the span gas values was calculated for each measurement cycle.
4. A linear regression equation was used to model this correction factor as a function of total water vapour mixing ratio for each cycle.
5. The appropriate correction factor was then applied to the 10 Hz raw data.
6. Finally, new isotopic mixing ratios were calculated for flux computations.

3.4 Eddy-Covariance Instrumentation

Wind velocity fluctuations were measured at 10 Hz using a three-dimensional sonic anemometer-thermometer (CSAT3, CSI). Total water vapour fluctuations were measured at 10 Hz using the TDL and open and closed-path infrared gas analyser (IRGA) (models LI7500 and LI7000, Licor Inc., Nebraska, USA). The closed-path IRGA was maintained in a temperature-controlled housing (TCH, Model GA-TCH, Biometeorology and Soil Physics Group, University of British Columbia, British Columbia, Canada). Air was pulled through the analyser at a flow rate of 10 l min^{-1} and the sample cell pressure was maintained at 65 kPa. All eddy fluxes were calculated from 30- min block averaging followed by a two-dimensional coordinate rotation.

3.5 Liquid Water Isotope Analysis

Liquid water, including precipitation, soil, xylem, and the dripper calibration water, were analyzed using a distributed feedback (DFB, near-infrared) tunable diode laser with off-axis integrated-cavity-output spectroscopy (DLT-100, Los Gatos Research Inc., Mountain View, California, USA) (Lis et al. 2008). The DLT-100 was integrated with an autosampler

(HT300A, HTA Srl, Brescia, Italy) using an embedded National Instruments controller (cFP-2120, National Instruments, Austin, Texas) to translate the communications. Soil and xylem water were extracted on a custom designed glass vacuum line. All water isotope analyses were conducted by running each sample six times to reduce memory effects. We rejected the first three measurements and used the final three measurements to characterize the isotope ratio of each sample. For each run, water standards were chosen to bracket the expected values for that set of unknown samples. In some cases, samples were re-analysed to provide an optimal set of calibration standards. Typical precision was 0.2‰ for $\delta^{18}O$. Research has demonstrated excellent agreement between these relatively new optical isotope techniques with traditional mass spectrometer methods (Brand et al. 2009). However, there is emerging evidence that organic contaminants can produce large errors in the measurement and care should be taken to identify such artifacts (Brand et al. 2009; West et al. 2010). We followed the sampling protocol proposed by the Moisture Isotopes in the Biosphere and Atmosphere (MIBA, http://ib.berkeley.edu/labs/dawson/MIBA-US/) program for sampling soil and xylem water. Xylem water was collected near midday (1200 LST) and samples were sealed in glass vials, wrapped with paraffin, and frozen until cryogenic water extraction on the glass line.

4 Results and Discussion

4.1 Evaluation of EC-TDL Performance

4.1.1 Precision and Accuracy

The precision of an earlier version of the TDL was reported previously by Lee et al. (2005) and Wen et al. (2008). Their results showed that the 25-s and 1-h average precision for $\delta^{18}O$ were 0.33 and 0.07‰, respectively when measured at a mixing ratio of 15.9 mmol mol^{-1}. Performance degraded slightly at lower water vapour mixing ratios. The short-term (10 Hz) noise of the TDL was determined under field conditions from the standard deviation of 10 Hz measurements when measuring a constant water vapour source (i.e. during calibration periods and measurement from a dew point generator). The 10 Hz noise values were typically 20.1 and 0.04 μmol mol^{-1} for $H_2^{16}O$ and $H_2^{18}O$ and 1.6‰ for $\delta^{18}O$. These noise values were compared to the measured water vapour fluctuations (i.e. the departures from the mean values over the calibration intervals, 10 or 12-min means) over a 3-day period (DOY 180–DOY 182, 2009) and indicated that the signal-to-noise ratios were 46 and 16 for $H_2^{16}O$ and $H_2^{18}O$, respectively. Compared to our EC-TDL CO_2 isotope application at the same site (Griffis et al. 2008), the signal-to-noise ratio was better by a factor of 2 to 3 for water vapour isotopes. Figure 5 provides an example of the 10 Hz fluctuations in w, sonic temperature (T_s), δ_v, and χ_w for a 10-min period near midday on DOY 184, 2009. These high frequency time series illustrate a number of key features including ramp structures that can be observed simultaneously in each of the traces. A lowpass filter (1-s running mean) applied to the 10 Hz δ_v signal indicates that its behaviour is strongly correlated with the other scalars (T_s and χ_w) and the atmospheric motion.

Following a similar approach to Lee et al. (2005), Wen et al. (2008), and Wang et al. (2009), we used a mixing ratio generator and the Rayleigh distillation model to evaluate the accuracy of the TDL system and our calibration technique described above. In this case, mixing ratios were generated in the laboratory using a custom designed mixing ratio

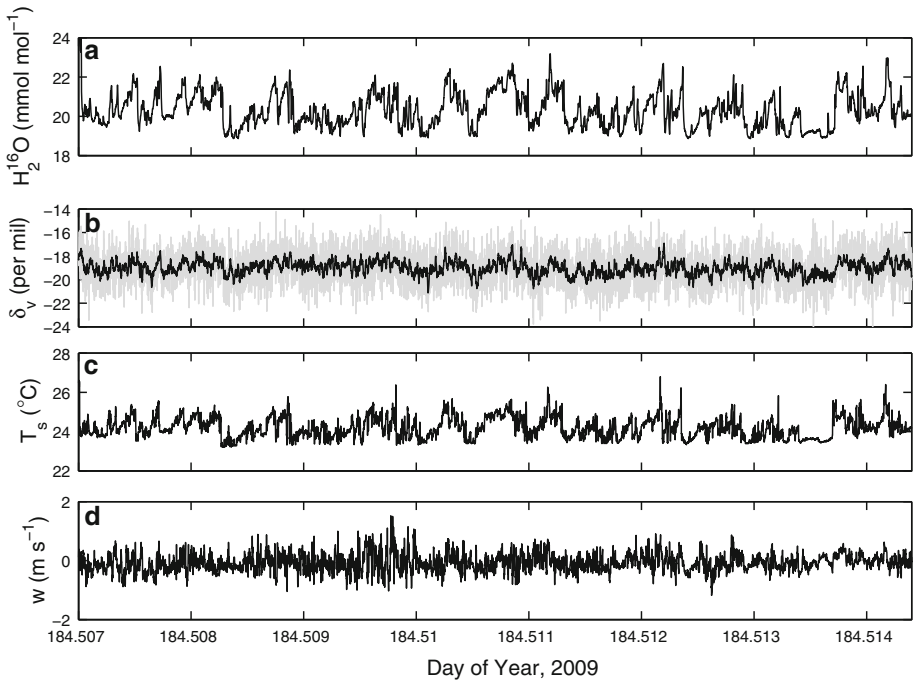

Fig. 5 Time series of high frequency (10 Hz) fluctuations of **a** $H_2^{16}O$ mixing ratio; **b** oxygen isotope composition of water vapour; **c** sonic temperature; **d** vertical wind velocity. The *gray trace* in **b** represents the calibrated 10 Hz signal. The *black trace* shows the effect of adding a low pass (1-s running mean) filter

generator that was developed specifically for generating water vapour with a known isotope ratio (Baker and Griffis 2010). The generator was filled with 20 ml of de-ionized water with known isotope ratio. Air from a compressed cylinder was passed through two molecular sieves and through the mixing ratio generator at a flow rate of approximately 0.5 l min^{-1}. The isotope ratio of the vapour (R_v) was predicted forward in time using the Rayleigh distillation model,

$$R_v = \frac{R_l}{\alpha}\left(\frac{m}{m_0}\right)^{1/\alpha - 1} \tag{6}$$

where R_l is the initial isotope ratio of water used to fill the dew point generator, m_0 is the initial mass of water, m is the residual mass of water in the vapour pressure generator, and α is the temperature-dependent equilibrium fractionation factor for oxygen-18 (Majoube 1971). The absolute isotope ratio of the water vapour (R_v) was converted to delta notation and compared directly with the TDL measurements. Figure 6 shows the laboratory Rayleigh test results for four different mixing ratios (18, 15, 12, and 9 mmol mol^{-1}) measured over a period of about 18–24 h. These data show good agreement between the measured and modelled $\delta^{18}O$ based on Rayleigh theory. The difference between the measured and predicted values at the end of the experiment was at best less than 0.14‰ and on average 0.89‰. The calculated isotopic ratio of the vapour in equilibrium with the liquid water is also shown for the beginning and end of each experiment as triangles (measured independently using the liquid water isotope analyser). The difference between these values and the TDL measurement was at best 0.09‰ and on average 0.50‰.

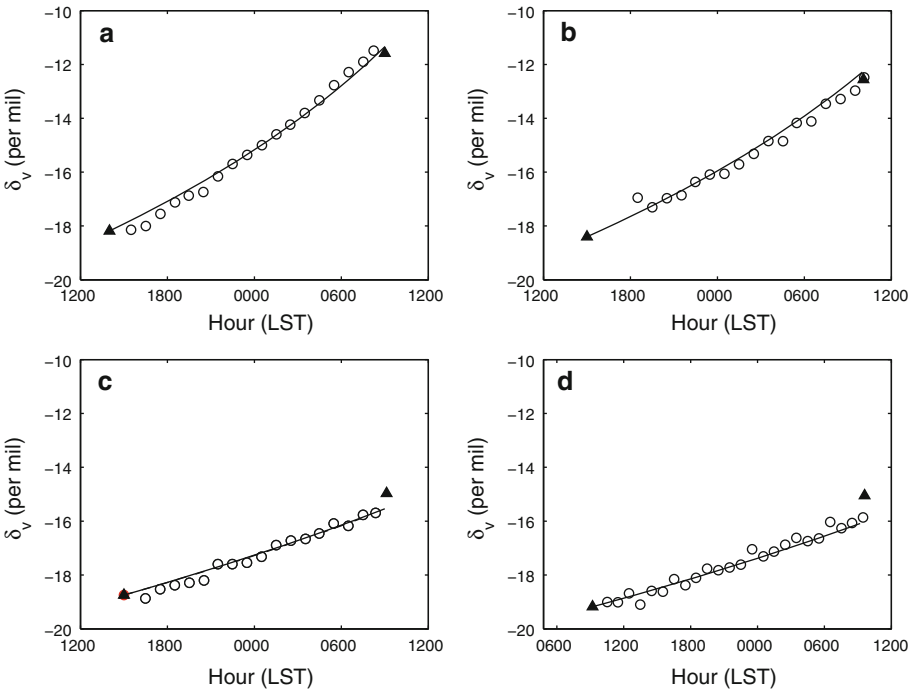

Fig. 6 Comparisons of the tunable diode laser water vapour isotope measurement versus values predicted from a Rayleigh distillation method. These tests were conducted under laboratory conditions over an 18–24 h period for mixing ratios (dew-point temperature) of: **a** 18 mmol mol^{-1} (15°C); **b** 15 mmol mol^{-1} (12°C); **c** 12 mmol mol^{-1} (9°C); and **d** 9 mmol mol^{-1} (4.6°C). *Triangles* indicate the calculated isotope ratio of the vapour in equilibrium with the liquid water at the beginning and end of the experiments. These end point values were measured using a distributed feedback tunable diode laser with off-axis integrated-cavity output spectroscopy

4.1.2 Linearity and Stability

Lee et al. (2005) showed that the tunable diode laser (TGA100) $\delta^{18}O$ sensitivity to water vapour mixing ratio was strongly non-linear. This presents an important challenge to measuring fluxes using the gradient or eddy-covariance approach. Their calibration strategy was to closely bracket (to within 10%) the ambient conditions using an upper and lower water vapour span value that was continuously adjusted based on an environmental feedback measurement loop. In the 2009 field experiment we adopted a similar strategy. Examples of the instrument $\delta^{18}O$ sensitivity to water vapour mixing ratio are shown for DOY 174 (Fig. 7a, b) and DOY 199 (Fig. 7c, d). The data points (solid circles) represent the median hourly values and the solid lines indicate the linear regression. Examples are shown for 0800 local standard time (upper panels) and 1600 local standard time (lower panels). The sensitivity of $\delta^{18}O$ to a change in mixing ratio was typically about 1‰ per mmol mol^{-1}. This non-linear response illustrates the importance of using the dynamic calibration. Previous studies have examined the calibration stability of the TDL for CO_2 and H_2O isotopes (Griffis et al. 2008; Wen et al. 2008). These studies demonstrated that the mixing ratio calibration precision was relatively stable for about 30- min and that the isotope ratio calibration precision was stable from about 1 h (H_2O) to nearly 3 h (CO_2) because the gain factor errors tended to be correlated.

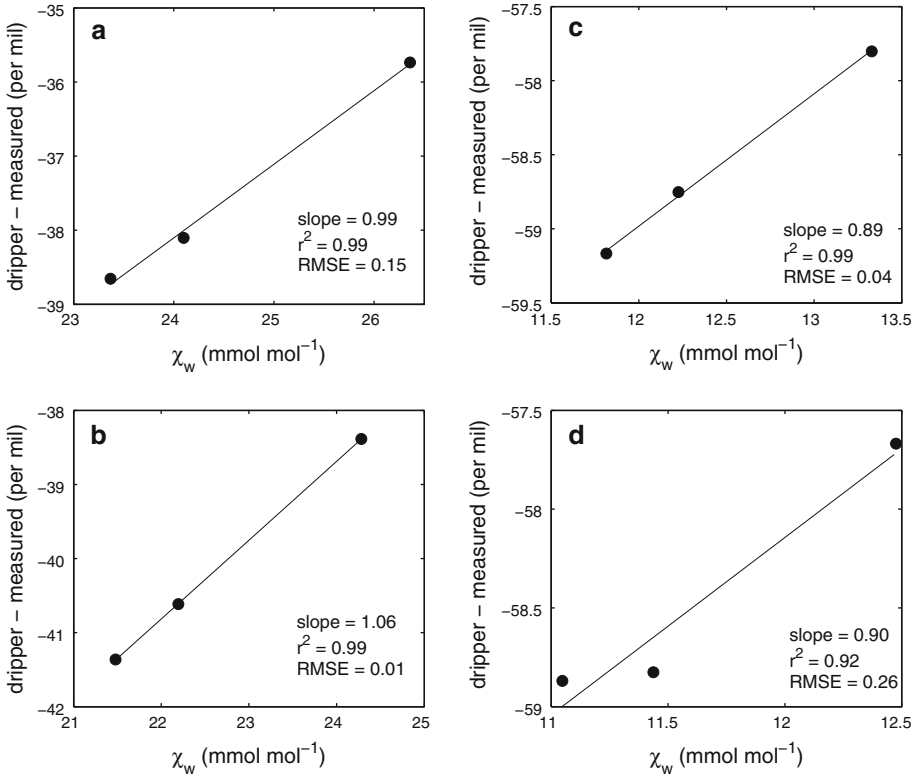

Fig. 7 Examples of the typical range of calibration correction factors and their dependence on the water vapour mixing ratio. The values shown are median hourly values for typical days during the 2009 corn field experiment. These values are corrected for a zero offset. A gain correction was not applied

4.1.3 Comparison of Tunable Diode Laser and Infrared Gas Analyser Measurements

A comparison of the total water vapour mixing ratio measured using the TDL and the open and closed-path IRGAs is shown in Fig. 8 (top panels) for the 2008 soybean experiment. In this case the TDL was calibrated at the beginning and end of the experimental period using a dew point generator. The water vapour mixing ratios were computed relative to the TDL reference cell mixing ratio. These results demonstrate relatively good agreement among each of the systems. There was slightly more scatter in the open-path IRGA because of its susceptibility to condensation/precipitation events and its calibration span value appeared to be low by approximately 10% compared to the closed-path IRGA. The linear regression equations for the TDL versus open-path IRGA and TDL versus closed-path IRGA were $y = 1.1x - 1.2$ ($r^2 = 0.92$ and RMSE = 1.05) and $y = 0.99x + 1.2$ ($r^2 = 0.99$ and RMSE = 0.30), respectively.

The time series of water vapour fluxes for each of the eddy-covariance systems is also shown in Fig. 8 (lower panels). In this case, we adjusted the open-path IRGA fluxes upward by 10% to account for the calibration span error. There was good agreement between the EC-TDL and EC-IRGA systems. The linear regression equations for the EC-TDL versus open-path EC-IRGA and the EC-TDL and closed-path EC-IRGA were $y = 0.99x - 0.01$

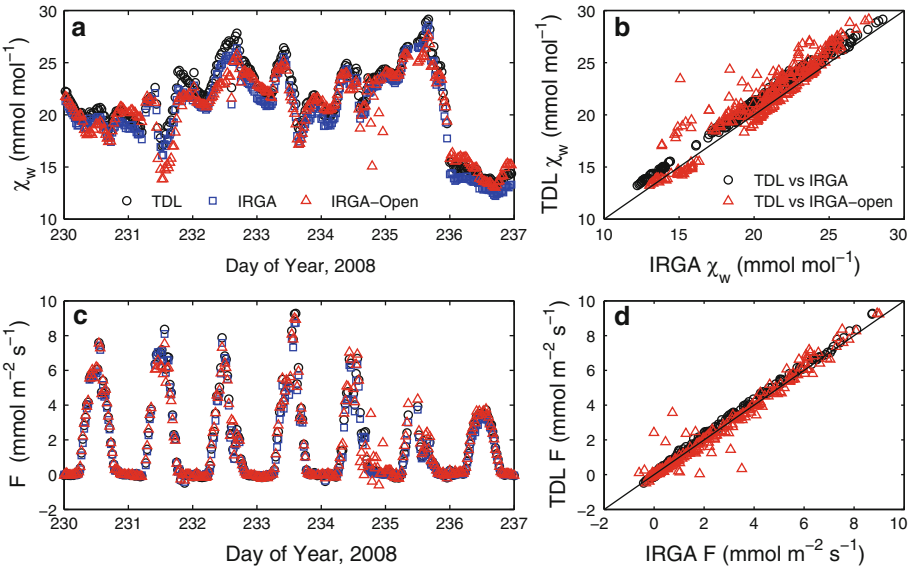

Fig. 8 Time series of water vapour mixing ratio measured with the TDL, IRGA, and open-path IRGA (**a**) and their 1:1 comparison (**b**); time series of the water vapour flux measured over the soybean canopy using eddy covariance based on three methods including the TDL, IRGA, and open-path IRGA (**c**) and their 1:1 comparison (**d**)

($r^2 = 0.997$ and RMSE = 0.11) and $y = 1.06x + 0.009$ ($r^2 = 0.999$ and RMSE = 0.058), respectively and indicate agreement to within about 6%. Although the frequency response of the EC-TDL system was lower at frequencies >0.6 Hz compared to the open-path IRGA (Fig. 9) it appears that the flux contribution (covariance) at these frequencies was not significant, resulting in an excellent comparison between these different measurement systems.

The midday spectral densities for $H_2^{16}O$, $H_2^{18}O$, and H_2O from an open and closed-path IRGA are shown in Fig. 9. All scalars (excluding deuterium) show a similar response at lower frequencies up to about 0.6 Hz. The TDL spectral response begins to diverge from that of the open-path IRGA beyond 1 Hz, falling to one-half at approximately 3 Hz. The TDL sample cell residence time is 130 ms, based on its volume (300 ml), flow (1.5 standard l min^{-1}), and pressure (1.1 kPa). Assuming there is no mixing in the sample cell, and no attenuation of high frequencies in the tubing or other sampling system components, the ideal half-power response frequency is 3.4 Hz. This good agreement between the ideal and measured frequency response shows there is very little mixing in the sampling system or TDL. In contrast, the residence time of the closed-path IRGA sample cell is 42 ms, based on its volume (10.9 ml), flow (10 standard l min^{-1}), and pressure (65 kPa), giving it an ideal frequency response of 10.5 Hz. The measured response of the closed-path IRGA falls to half that of the open-path IRGA at approximately 1.5 Hz, much worse than expected. This comparison indicates the frequency response of the closed-path IRGA is dominated by mixing in the analyser, tubing, or other sampling system components.

It is also important to note the similar behaviour between the two isotopes ($H_2^{16}O$ and $H_2^{18}O$), which provides evidence that any tube attenuation is similar for both species. This suggests, therefore, that kinetic fractionation resulting from tubing effects is not likely to be significant at these high flow rates/Reynolds numbers. This is further supported by the fact that the maximum covariance between these isotopes and the vertical wind fluctuations was

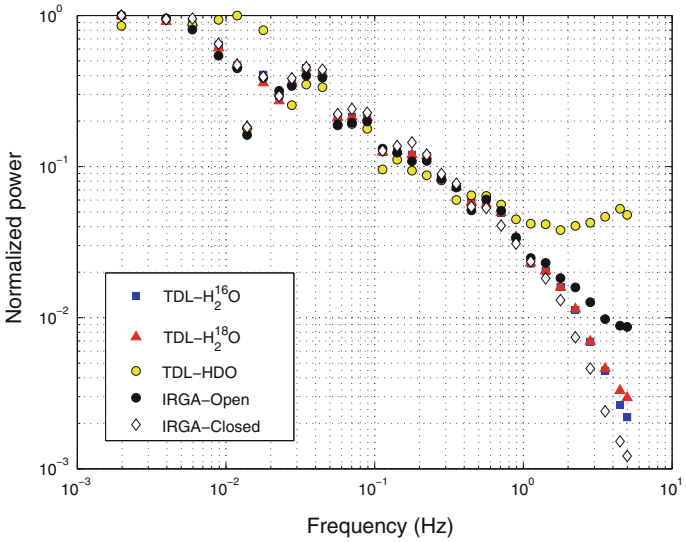

Fig. 9 Spectral density analysis. Normalised spectrum of TDL and IRGA 10 Hz time series over a 3-h period (1200–1500 local time) on DOY 228, 2008 soybean canopy. Spectra were computed at 10- min intervals using Welch's averages periodogram method using Matlab. The spectra were bin averaged using 10 logarithmically spaced intervals per decade. Wind direction was 150° from north and wind speeds were approximately 1.5 m s^{-1}. F ranged between 8 and 9 mmol m^{-2} s^{-1}

found with the same median lag factor (≈1.7 s) and so were highly correlated ($r = 0.999$). The potential kinetic fractionation effect resulting from tube attenuation was also found to be negligible for CO_2 isotopes (Griffis et al. 2008). While deuterium is not the focus of our study, Fig. 9 indicates that the spectral density of deuterium is more variable, which may be a consequence of tube attenuation. The lag factor associated with the maximum covariance between vertical wind fluctuations and deuterium was highly variable and poorly correlated ($r = 0.349$) with $H_2^{16}O$, and may be related to both tubing effects and low signal-to-noise ratio. Finally, the spectral densities of δH and δ^{18} (Fig. 10) indicate that the noise increases significantly at frequencies above 1.4 Hz. The δH spectrum shows greater variability than δ^{18} and the response falls far below it at about 0.4 Hz suggesting that there is a greater tube effect on deuterium.

4.1.4 Discrimination Patterns and Processes

Fast measurement of the water vapour isotopes should provide new insights regarding the nature of turbulent transport of water vapour between the surface and atmosphere. We hypothesise that different scales of turbulent motion in the boundary layer would have distinct or persistent isotopic signatures. Small scales of motion may bear an isotopic signal more characteristic of the vegetation/canopy. Larger organised scales of motion, which are relatively long-lived, may be linked to entrainment processes and/or penetration deep into the canopy layer. In such cases the isotopic signal would be significantly different than the canopy or the average isotope flux ratio. Figure 11 shows the normalised cospectra for temperature and the water vapour isotopes for July 7, 2009 over the corn canopy (1200–1800 LST). The top panel illustrates that there is cospectral similarity among the sensible heat and water

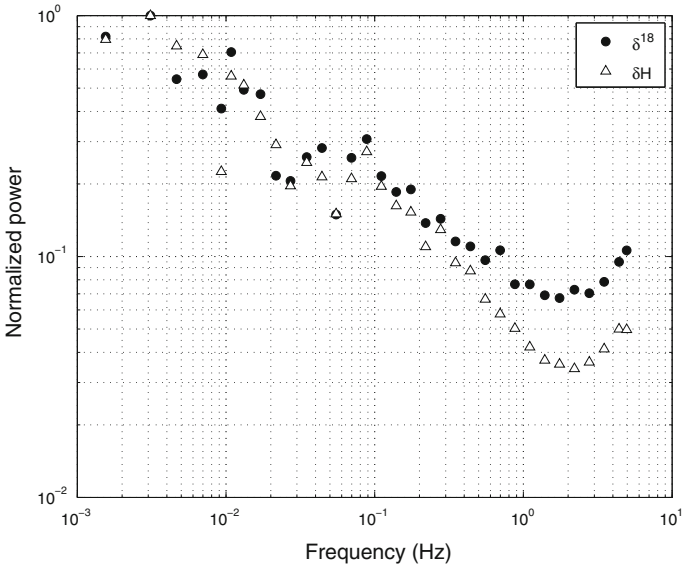

Fig. 10 Spectral density analysis. Normalised spectrum of δH and δ^{18} 10 Hz time series over a 3-h period (1200–1500 local time) on DOY 196, 2009 corn canopy. Spectra were computed at 12-min intervals using Welch's averages periodogram method using Matlab. The spectra were bin averaged using 10 logarithmically spaced intervals per decade. Wind direction was 260° from north and wind speeds were approximately 4.0 m s^{-1}. F ranged between 3 and 4 mmol m^{-2} s^{-1}

vapour isotopic fluxes. Further, it illustrates that the majority of the flux transport can be attributed to frequencies between about 1 and 0.0062 Hz. The lower panel shows an example of the cospectral flux ratio. Three features should be noted. First, at the very high and low frequencies (2 Hz $< f <$ 0.0062 Hz) where the flux contribution is small, the flux isotope ratio is very noisy. Second, the frequencies most important for flux transport have an isotopic composition that fluctuates between -7 and -5‰. This compares favourably with the measured isotopic ratio of the extracted corn xylem water ($\delta_x = -7.1$‰) and the soil water ($\delta_s = -5.3$‰ at 0.1 m depth) for midday on July 7, 2009. During this time period the leaf area index was ≈2.0 and midday soil evaporation, measured with an automated chamber system, represented less than 6% of evapotranspiration. Assuming steady-state conditions during midday to late afternoon, we expect that $\delta_F \approx \delta_x$ (Lee et al. 2007; Welp et al. 2008). It appears from Fig. 11 that this condition is satisfied for some scales of motion. Departures from δ_x during this time period represent differences in sources as related to the scales of atmospheric motion/transport or in some instances may be an artifact of the instrument noise.

Figure 12 shows the diurnal ensemble patterns of δ_v, F, δ_F, and I_F for the corn canopy June (black circles), July (blue squares), and August (red triangles) 2009. The isotopic composition of water vapour was relatively more depleted during peak canopy growth, ranging from about -18‰ at night to about -20‰ before midday. Similar patterns were reported by Welp et al. (2008) and are directly related to variations in synoptic meteorology. F_v was similar for June, July, and August, with mean maximum values of about 5.5 mmol m^{-2} s^{-1} in June. The ensemble patterns of δ_F show progressive ^{18}O enrichment through the day ranging from about -20‰ before sunrise to about -5‰ in late afternoon. Nighttime values were highly variable and depended on the formation and presence of dew. If dew events were filtered from the dataset, δ_F values were generally more positive at night (up to 20 or 30‰).

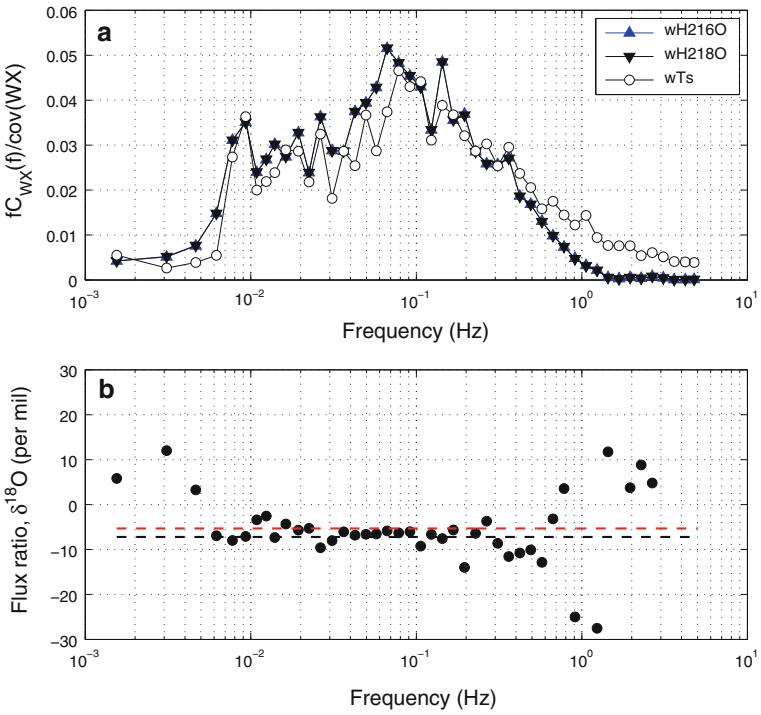

Fig. 11 Normalised cospectrum for temperature and water vapour isotopes (**a**) and investigation of isotope ratio spectral similarity (**b**). The isotopic composition of the water vapour flux was computed from the ratio of cospectral densities and plotted in delta notation (‰) as a function of frequency. The *thick black dashed line* indicates the isotope ratio of the corn xylem water, $\delta_x = -7.1$‰. The *thick dashed red line* indicates the isotope ratio of the soil water, $\delta_s = -5.3$‰ measured at a depth of 0.1 m. Data are shown for DOY 188, 2009

The values of δ_F were similar to δ_x values (-7.2‰) for only short periods of time from about 1400 to 1800 LST, indicating near steady-state conditions.

The influence of soil evaporation on δ_F was minor since soil evaporation was typically less than 10% during midday. Soil water extraction from a depth of 0.1 m indicated that the soil water isotope composition was on average, -5.4, -3.9, and -6.2‰ for June, July, and August, respectively. Therefore, based on the isotopic mass balance we calculated that the isotopic composition of transpiration was slightly more enriched (0.2–0.6‰) compared to δ_F. This small difference indicates that δ_F is a close approximation of the transpiration isotope signal. During the 2009 measurement period (about 74 days), the flux-weighted δ_F ranged from -9.6 to -7.2‰ and was within the bounds of the local ground water and precipitation isotopic ratio.

Finally, the isotopic forcing values and patterns shown in Fig. 12 are in excellent agreement with those reported previously by Welp et al. (2008). It is interesting to note that the isoforcing is nearly always positive, yet the δ_v values do not reveal significant daytime enrichment. These patterns suggest that the isoforcing related to boundary-layer growth and entrainment is very strong and has a dominant influence on surface-layer air. As shown by the modelling and measurement analyses of Xiao et al. (2010), isoforcing associated with ^{18}O–CO_2 is dependent on relative humidity. Figure 13 provides additional support for this relationship and indicates that higher relative humidity acts to lower the water vapour isoforcing. The relation

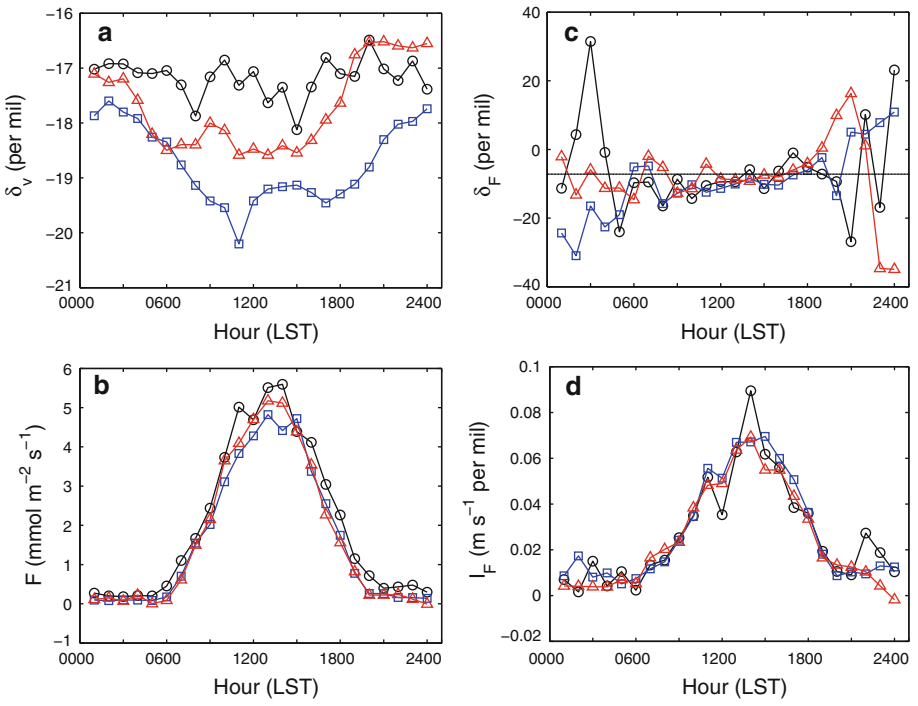

Fig. 12 Diurnal patterns of δ_v, F, δ_F, and I_F for June (*black circles*), July (*blue squares*), and August (*red triangles*), 2009 corn growing season. The horizontal line in panel **c** indicates the mean isotope ratio of the xylem water

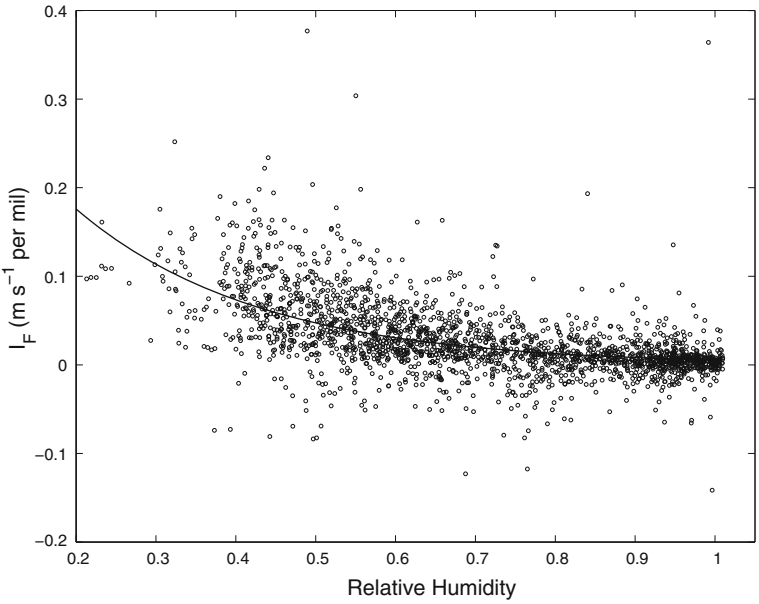

Fig. 13 The influence of relative humidity on the isotopic forcing (I_F) during the 2009 growing period. The values shown are half-hourly values for the growing season. Here, relative humidity is referenced to the canopy temperature

can be described with a simple exponential function ($y = 0.422e(-4.4RH)$, $r^2 = 0.68$, RMSE = 0.02) and is intimately connected to the ^{18}O–CO_2 exchange between the biosphere and atmosphere (Xiao et al. 2010). These patterns and processes are being investigated in greater detail to help understand the oxygen isotope composition of evapotranspiration and its relation to C_4 ^{18}O–CO_2 photosynthetic discrimination. The ability to quantify these fluxes and discrimination factors at the canopy scale are expected to help provide the fundamental data needed to develop and validate land-surface models that consider isotopic budgets of both water and carbon (Xiao et al. 2010).

5 Conclusions

Eddy covariance and tunable diode laser spectroscopy were combined to measure the oxygen isotope composition of evapotranspiration and the isotopic forcing on surface-layer air. Total water vapour mixing ratio and fluxes with traditional eddy-covariance and infrared gas analysers were in good agreement with the eddy-covariance tunable diode laser technique. There did not appear to be a significant phase shift among isotopes or kinetic fractionation caused by the tube attenuation. The isotope composition of evapotranspiration was in close agreement with the isotope composition of the corn xylem water in late afternoon indicating near steady-state conditions. The diurnal patterns in the isotopic fluxes, isotopic forcing, and their functional relationship with relative humidity provide strong evidence that the methodology is robust and shows considerable promise for long-term continuous measurements under field conditions. The broader application of this technique should provide new insights regarding water and carbon cycle processes and should increase the power of the ^{18}O–H_2O and ^{18}O–CO_2 isotope tracers.

Acknowledgements This work is dedicated to the memory of Bert Tanner who helped pioneer tunable diode laser spectroscopy techniques for micrometeorological research. We express our sincere thanks to Jeremy Smith and Bill Breiter for their technical assistance in the lab and at the field site. Funding for this research has been provided by the National Science Foundation, ATM-0546476 (TG), ATM-0914473 (XL), DEB-0514908 (XL and TG), the Office of Science (BER) U.S. Department of Energy, DE-FG02-06ER64316 (TG and JB) and the College of Food, Agricultural and Natural Resource Sciences, at the University of Minnesota.

References

Angert A, Lee JE, Yakir D (2008) Seasonal variations in the isotopic composition of near-surface water vapour in the eastern mediterranean. Tellus 60:674–684

Baker JM, Griffis TJ (2010) A simple, accurate, field-portable mixing ratio generator and Rayleigh distillation device. Agric For Meteorol (in press)

Bowling DR, Delany AC, Turnipseed AA, Baldocchi DD, Monson RK (1999) Modification of the relaxed eddy accumulation technique to maximize measured scalar mixing ratio differences in updrafts and downdrafts. J Geophys Res 104(D8):9121–9133

Bowling DR, Tans PP, Monson RK (2001) Partitioning net ecosystem carbon exchange with isotopic fluxes of CO_2. Glob Change Biol 7(2):127–145

Brand W, Geilmann H, Crosson E, Rella C (2009) Cavity ring-down spectroscopy versus high-temperature conversion isotope ratio mass spectrometry; a case study on delta h-2 and delta o-18 of pure water samples and alcohol/water mixtures. Rapid Commun Mass Spectrom 23:1879–1884

Brown D, Worden J, Noone D (2008) Comparison of atmospheric hydrology over convective continental regions using water vapor isotope measurements from space. J Geophys Res 113(D15). doi:10.1029/2007JD009676

Griffis TJ, Baker JM, Sargent SD, Tanner BD, Zhang J (2004) Measuring fieldscale isotopic CO_2 fluxes with tunable diode laser absorption spectroscopy and micrometeorological techniques. Agric For Meteorol 124(1–2):15–29

Griffis TJ, Lee X, Baker JM, Sargent SD, King JY (2005) Feasibility of quantifying ecosystem-atmosphere $C^{18}O^{16}O$ exchange using laser spectroscopy and the flux-gradient method. Agric For Meteorol 135(1–4):44–60

Griffis TJ, Sargent SD, Baker JM, Lee X, Tanner BD, Greene J, Swiatek E, Billmark K (2008) Direct measurement of biosphere–atmosphere isotopic CO_2 exchange using the eddy covariance technique. J Geophys Res 113:D08304. doi:10.1029/2007JD009297

He H, Smith R (1999) Stable isotope composition of water vapor in the atmospheric boundary layer above the forests of new England. J Geophys Res 104:11657–11673

Herbin H, Hurtmans D, Turquety S, Wespes C, Barret B, Hadji-Lazaro J, Clerbaux C, Coheur PF (2007) Global distributions of water vapour isotopologues retrieved from IMG/ADEOS data. Atmos Chem Phys 7(14):3957–3968

Jacob H, Sonntag C (1991) An 8-year record of the seasonal-variation of H-2 and O-18 in atmospheric water-vapor and precipitation at Heidelberg, Germany. Tellus 43B(3):291–300

Lai C, Ehleringer J, Bond B, Paw UKT (2006) Contributions of evaporation, isotopic non-steady state transpiration and atmospheric mixing on the delta O-18 of water vapour in Pacific Northwest coniferous forests. Plant Cell Environ 29(1):77–94

Lee X, Sargent S, Smith R, Tanner B (2005) In-situ measurement of the water vapor $^{18}O/^{16}O$ isotope ratio for atmospheric and ecological applications. J Atmos Ocean Technol 22:555–565

Lee XH, Kim K, Smith R (2007) Temporal variations of the $^{18}O/^{16}O$ signal of the whole-canopy transpiration in a temperate forest. Glob Biogeochem Cycles21(3):GB3013. doi:10.1029/2006GB002871

Lee X, Griffis T, Baker J, Billmark K, Kim K, Welp L (2009) Canopy-scale kinetic fractionation of atmospheric carbon dioxide and water vapor isotopes. Glob Biogeochem Cycles 23:GB1002. doi:10.1029/2008GB003331

Lis G, Wassenaar LI, Hendry MJ (2008) High-precision laser spectroscopy D/H and O-18/O-16 measurements of microliter natural water samples. Anal Chem 80(1):287–293. doi:10.1021/ac701716q

Majoube M (1971) Fractionnement en oxygene-18 et en deuterium entre l'eau et sa vapeur. J Chim Phys 68:1423–1436

Sturm P, Knohl A (2009) Water vapor δ^2H and δ^{18}O measurements using off-axis integrated cavity output spectroscopy. Atmos Meas Tech Discuss 2:2055–2085

Wang L, Caylor K, Dragoni D (2009) On the calibration of continuous, high-precision δ^{18}o and δ^2h measurements using an off-axis integrated cavity output spectrometer. Rapid Commun Mass Spectrom 23:530–536

Welp LR, Lee X, Kim K, Griffis TJ, Billmark KA, Baker JM (2008) δ^{18}O of water vapour, evapotranspiration and the sites of leaf water evaporation in a soybean canopy. Plant Cell Environ 31(9):1214–1228. doi:10.1111/j.1365-3040.2008.01826.x

Wen XF, Sun XM, Zhang SC, Yu GR, Sargent SD, Lee X (2008) Continuous measurement of water vapor D/H and O-18/O-16 isotope ratios in the atmosphere. J Hydrol 349(3–4):489–500. doi:10.1016/j.jhydrol.2007.11.021

West AG, Goldsmith G, Brooks P, Dawson T (2010) Discrepancies between isotope ratio infrared spectroscopy and isotope ratio mass spectrometry for the stable isotope analysis of plant and soil waters. Rapid Commun Mass Specrom 24:1948–1954

Worden J, Bowman K, Noone D, Beer R, Clough S, Eldering A, Fisher B, Goldman A, Gunson M, Herman R, Kulawik SS, Lampel M, Luo M, Osterman G, Rinsland C, Rodgers C, Sander S, Shephard M, Worden H (2006) Tropospheric emission spectrometer observations of the tropospheric HDO/H_2O ratio: estimation approach and characterization. J Geophys Res 111(D16). doi:10.1029/2005JD006606

Worden J, Noone D, Bowman K (2007) Importance of rain evaporation and continental convection in the tropical water cycle. Nature 445(7127):528–532

Xiao W, Lee X, Griffis T, Kim K, Welp L, Yu Q (2010) A modeling investigation of canopy-air oxygen isotopic exchange of water vapor and carbon dioxide in a soybean field. J Geophys Res 115:G01004. doi:10.1029/2009JG001163

Yakir D, Wang XF (1996) Fluxes of CO_2 and water between terrestrial vegetation and the atmosphere estimated from isotope measurements. Nature 380(6574):515–517